

Theory of relaxation oscillations in exciton-polariton condensatesAndrzej Opala,^{1,*} Maciej Pieczarka,² and Michał Matuszewski¹¹*Institute of Physics, Polish Academy of Sciences, Al. Lotników 32/46, 02-668 Warsaw, Poland*²*OSN, Department of Experimental Physics, Faculty of Fundamental Problems of Technology, Wrocław University of Science and Technology, W. Wyspiańskiego 27, 50-370 Wrocław, Poland*

(Received 14 June 2018; revised manuscript received 3 November 2018; published 26 November 2018)

We provide an analytical and numerical description of relaxation oscillations in the nonresonantly pumped polariton condensate. Presented considerations are based on coupled rate equations that are derived from the open dissipative Gross-Pitaevskii model. The evolution of the condensate density can be explained qualitatively by studying the topology of the trajectory in phase space. We use a fixed points analysis for the classification of the different regimes of condensate dynamics, including fast stabilization, slow oscillations, and ultrashort pulse emission. We obtain an analytical condition for the occurrence of relaxation oscillations. Continuous and pulsed condensate excitations are considered and we demonstrate that, in the latter case, the existence of the second reservoir is necessary for the emergence of oscillations. We show that relaxation oscillations should be expected to occur in systems with relatively short polariton lifetimes.

DOI: [10.1103/PhysRevB.98.195312](https://doi.org/10.1103/PhysRevB.98.195312)**I. INTRODUCTION**

Exciton-polaritons, coherently coupled excitons, and photons in a semiconductor microcavity [1,2] enabled the creation of a class of bosonic condensates characterized by nonequilibrium dissipative nature and complex nonlinear dynamics. The unique properties of polariton quantum fluids bring the possibility to observe phenomena of superfluidity, instability, self-localization, self-trapped magnetic polarons, topological and nonlinear excitations [3–16]. Describing polariton dynamics is an interesting physical problem important for the fundamental description of light-matter condensation and potential polaritonic applications [17–19]. In this paper, we focus on the theoretical description of the nontrivial time evolution of polariton quantum fluid characterized by oscillatory behavior.

To date, oscillations of emission intensity in polariton systems have been investigated in several different contexts. The common phenomenon occurring in the case of resonant excitation is the Rabi oscillations between photonic and excitonic component of polaritons [20–22]. Spatial or spin oscillatory dynamics of exciton-polariton condensates were assigned in several works to the coupling of condensates forming an analog of a superconductor Josephson junction [23–26]. Josephson oscillations take place between two macroscopic bosonic ensembles occupying single macroscopic states separated by tunnel barrier. The nontrivial polariton density oscillation in space was also studied in the context of Zitterbewegung effect [27].

Relaxation oscillations observed in polariton condensates have a completely different character than Rabi or Josephson oscillations, since there is no periodic transfer of particles between components constituting the polariton fluid. Instead, relaxation oscillations are due to periodic change in the

efficiency of relaxation from the reservoir of uncondensed particles to the condensate, and may even take the form of sharp spikes, well separated in time. From the point of view of the excitation spectrum, such oscillations correspond to complex frequencies with a nonzero real part in the limit of zero momentum in the Bogoliubov dispersion. This is in contrast to purely imaginary frequencies found in the cases considered in Ref. [26]. The first experimental observation of relaxation oscillation in polariton system was reported in Ref. [28]. The oscillatory behavior was also studied in Ref. [29] and in the context of ultrashort emission of pulses from polariton condensate propagating in a disordered potential [30].

From the general point of view, relaxation oscillations are a family of periodic solutions occurring in various dynamical systems. Mathematically, this type of dynamics can be observed in a certain class of coupled nonlinear differential equations. The most well-known examples are the oscillating electrical triode circuits and B-class semiconductor lasers [31–33]. These systems can be described by a nonlinear Van der Pol equation. One of the characteristic properties of relaxation oscillations is the possibility of the presence of two stages in the cycle possessing different timescales [34]. The first timescale is related to a slow change of phase and the second timescale represents rapid change due to a fast relaxation. Following this rapid change, the system can return to the stage of slow evolution [34].

Here, we study relaxation oscillations in an exciton-polariton condensate analytically and numerically using a model including both an inactive and active reservoir coupled to the polariton condensate. We derive a second-order differential equation for the condensate density, applicable in the regime of continuous and pulsed nonresonant excitation. We analyze the solutions to this equation in linear and nonlinear regimes, and demonstrate that the oscillatory character of nonlinear fixed points explains the existence of relaxation oscillations in a certain parameter range. In the case of pulsed

*opala@ifpan.edu.pl

excitation, we find that the existence of the inactive reservoir is crucial for the appearance of oscillations. An analytical condition for the oscillatory regime is derived, which provides results consistent both with numerical simulations and with previous experimental observations.

The paper is structured as follows. In Sec. II, we define the model based on the rate equations derived from the mean-field open-dissipative Gross-Pitaevskii equation (ODGPE). In Sec. III, we investigate numerically the oscillatory evolution of the condensate. We describe in detail the mechanism of relaxation oscillations, considering the stimulated scattering and evolution of the reservoirs. In Sec. IV, we analyze the fixed points of the model and the system time evolution in phase space. We derive an analytical condition for the existence of relaxation oscillations. Section V summarizes our work.

II. MODEL

Modelling exciton-polariton condensates excited nonresonantly is a complex problem. In many cases, theoretical reconstruction of the experimental data must take into account processes of exciton reservoir formation, their relaxation, and stimulated scattering to the condensate. In our work, we consider the evolution of two reservoirs called the active and inactive reservoir [4,35]. The physical interpretation of these two reservoirs may differ in different experimental conditions. For example, in Ref. [28] the two reservoirs were attributed to excitons residing in the vicinity of the localized condensate and away from it. On the other hand, in Refs. [36,37] the two components of dynamics were identified as the reservoir of excitons and free carriers (electron-hole plasma). Here, we do not specify the exact nature of the two fields, but assume that the system can be roughly divided into two sets of excitations and only the active reservoir modes provide direct stimulated scattering to the polariton condensate. Importantly, as we will show below, taking into account the second reservoir is necessary for the existence of oscillations in the case of pulsed excitation, which is relevant to recent experiments [28,30].

The considered system can be modelled using the ODGPE and rate equations written, respectively, for both reservoirs. The ODGPE describes the temporal evolution of the complex polariton order parameter $\Psi(\mathbf{r}, t)$. This equation is dynamically coupled to the rate equation for the active reservoir $n_R(\mathbf{r}, t)$. We also include the equation describing population of the inactive reservoir $n_I(t)$ generated by the nonresonant laser field. The equations take the form presented below:

$$i\hbar \frac{\partial \Psi}{\partial t} = \left[-\frac{\hbar^2}{2m^*} \nabla^2 + \frac{i\hbar}{2} (Rn_R - \gamma_C) + U \right] \Psi, \quad (1)$$

$$\frac{\partial n_R}{\partial t} = \kappa n_I^2 - \gamma_R n_R - Rn_R |\Psi|^2, \quad (2)$$

$$\frac{\partial n_I}{\partial t} = P - \kappa n_I^2 - \gamma_I n_I, \quad (3)$$

where m^* is the effective mass of lower polaritons and $P(\mathbf{r}, t)$ is the laser pumping rate. The scattering into the reservoir and stimulated scattering rate into the condensate are described by κ and R . We assume that the scattering from the inactive reservoir and the stimulated relaxation of polaritons are respectively given by the function $\kappa n_I(\mathbf{r}, t)^2$ and the function

$n_R(\mathbf{r}, t)R$. While the form of scattering terms may be different for a particular physical interpretation, the results presented in this paper would not change qualitatively. The losses in the system are characterized by the parameters γ_I , γ_R , and γ_C describing the decay of inactive and active reservoirs and decay of polaritons, respectively. The decay rate of polaritons γ_C incorporates the finite lifetime of the photon component in semiconductor microcavity and the none-radiative decay rate of excitons. The potential $U(\mathbf{r}, t)$ is the effective potential composed of the static potential due to sample design or disorder, the mean-field interaction within the condensate, and between the condensate and reservoirs.

In our work, we will limit our considerations to the case when the condensate is practically trapped in a potential well, in which case it is possible to use simplified single-mode approximation to the condensate dynamics. We will use the same approximation to the reservoir fields, although allowing that the active and inactive reservoir may possess different spatial distributions than the condensate, as suggested in Refs. [28,38]. Nevertheless, we will neglect any changes of spatial distributions during the oscillations, which, however, still allows us to describe the main physics behind these phenomena. The reduced set of rate equations is the starting point of our work, and reads

$$\begin{aligned} \frac{dn_C}{dt} &= Rn_R n_C - \gamma_C n_C, \\ \frac{dn_R}{dt} &= \kappa n_I^2 - \gamma_R n_R - Rn_R n_C, \\ \frac{dn_I}{dt} &= P(t) - \kappa n_I^2 - \gamma_I n_I. \end{aligned} \quad (4)$$

In our considerations, we will consider in detail two limiting cases, the continuous wave pumping where $P(t) = \text{const}$ and ultrashort pulse pumping where $P(t) = P_0 \delta(t)$.

III. RESULTS

For clarity, we begin our presentation with an example of relaxation oscillations in the case of continuous wave excitation. We solved both the full model Eqs. (1)–(3) and Eqs. (4) numerically with a fourth-order Runge-Kutta method. Exemplary results are presented in Fig. 1. The details of simulation parameters are given in Table I in the Appendix. To obtain complex and relevant polariton condensate dynamics, we used parameter values similar to the ones used in the experimental works [28,30]. In particular, we chose a short polariton lifetime with respect to the exciton reservoir decay rate, which was inspired by the observation that the oscillating dynamics appears naturally in lower quality microcavities [28,30]. Initially, the reservoir fields are assumed to be empty and the condensate density is seeded with a small nonzero value, so that condensate formation buildup is possible. We assume that such a small seed may result from thermal or quantum fluctuations in the polariton field, but the investigation of its origins is beyond this paper. We emphasize that the results do not depend qualitatively on the value of the initial seed.

As shown in Fig. 1, initially the nonresonant pumping generates the population in the inactive reservoir n_I , which builds

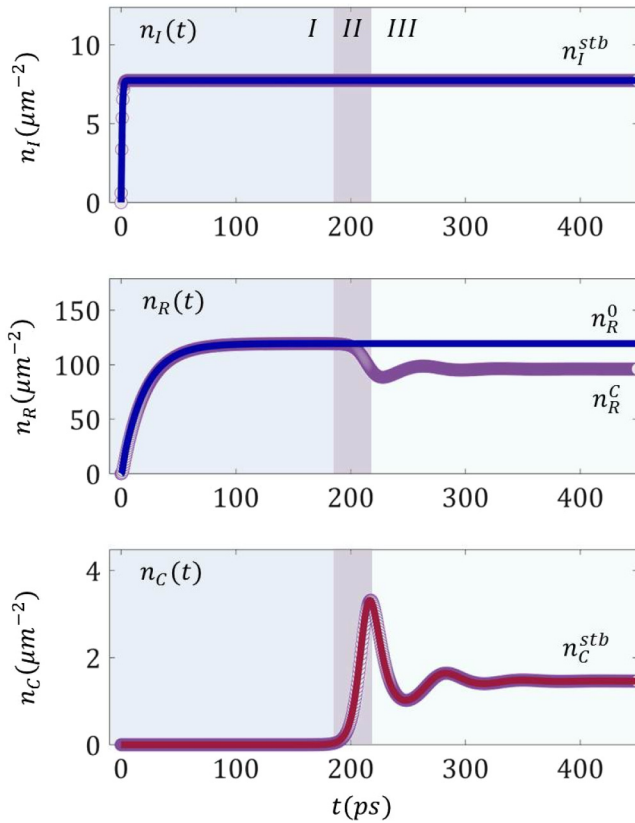


FIG. 1. Time evolution of polariton population $n_C(t)$ and incoherent reservoirs $n_I(t)$ and $n_R(t)$ generated by continuous wave excitation. Blue lines correspond to the analytical solution describing the evolution of reservoirs under the assumption of negligible polariton population. Red line presents condensate evolution obtained by nonlinear oscillator approximation, Eqs. (4). Grey points correspond to numerical solution obtained from the full open-dissipative Gross-Pitaevskii Eqs. (1)–(3). Condensate parameters are given in Table I.

up quickly and saturates at a stationary level. The long-lived inactive reservoir relaxes and feeds the active reservoir. The active reservoir density is increased up to a level determined by the stationary value n_R^0 and the condensate density is negligibly small. This phase of dynamics is marked as stage I in Fig. 1.

Next, the increasing density of the exciton reservoir results in accumulation of the polariton condensate density due to the stimulated relaxation process. The polariton field grows exponentially. This short phase of condensate dynamics is presented as stage II in Fig. 1.

The relaxation oscillations in the condensate develop when the rapid condensate density growth stops due to the resulting depletion of the active reservoir. In stage III in Fig. 1, the system is described by two timescales. The first timescale is related to the fast oscillations and the condensate decay rate. The second timescale is slower and it is related to the active reservoir decay. In each cycle of oscillations, the active reservoir density is initially depleted by the strong scattering to the condensate. The decreased reservoir density cannot sustain the condensate, which leads to fast decay of the polariton field, due to its large decay rate γ_C . In the second stage of the cycle, the reduced stimulated scattering allows

the active reservoir to be replenished. In effect, the minima and maxima of reservoir and condensate density are shifted in time with respect to each other by one-quarter of a cycle, see Fig. 1. These oscillations repeat until the condensate and reservoir reach the equilibrium level. It should be noted that in the single mode approximation, the numerical simulations of Equations (1)–(3) and Eqs. (4) give the same results. In the following sections, we focus only on the solution of rate Eqs. (4) for clarity.

A. Dynamics of reservoirs

To investigate quantitatively the oscillatory behavior of the polariton condensate, we determine the temporary dynamics of the inactive Eq. (2) and active reservoir Eq. (3). In the case of continuous wave condensate excitation, $P(t) = \text{const}$. The solution of Eq. (3) takes the form

$$n_I(t) = \frac{1}{2} \frac{\tanh\left(\frac{1}{2}t\sqrt{\eta^2 + \gamma_I^2 + \xi^0}\right)\sqrt{\eta^2 + \gamma_I^2 - \gamma_I}}{\kappa}, \quad (5)$$

where $\eta = \sqrt{4P_0\kappa}$ and $P_0 = \alpha P_{\text{th}}$. The parameter

$$\xi^0 = \tanh^{-1}\left(\frac{2n_I^{\text{in}}\kappa + \gamma_I}{\sqrt{\eta^2 + \gamma_I^2}}\right), \quad (6)$$

takes into account the initial level of inactive reservoir density n_I^{in} . When this reservoir is empty initially, i.e., when we consider turning on the pump abruptly with $(n_I(0) = n_I^{\text{in}} = 0)$ and $\gamma_I \ll \gamma_C, \gamma_R$, the parameter ξ^0 is negligibly small. The temporal evolution of $n_I(t)$ according to Eq. (5) is presented in Fig. 1 (top) with a blue solid line.

Typically, the population of the inactive reservoir given by Eq. (3) stabilizes relatively quickly after turning on the pump at $t = 0$. This is due to the asymptotic nature of the hyperbolic tangent solution of Eq. (6). The steady-state level of inactive reservoir density is obtained by equating the left-hand side of Eq. (3) to zero, which results in

$$n_I^{\text{stb}} = \frac{-\gamma_I + \sqrt{4\kappa P_0 + \gamma_I^2}}{2\kappa^{1D}}. \quad (7)$$

Stabilization of the inactive reservoir in stage I allows us to use the assumption that the inactive reservoir is constant during the subsequent stages (II, III) of evolution.

Next, we consider the dynamics of the active exciton reservoir n_R . We assume the absence of excitons in the active reservoir $n_R(0) = 0$ at the initial time. We consider two cases; that is, in the presence and absence of the condensate. These two types of dynamics have different solutions which also depend on the condensate density. First, we assume no polaritons in the condensate $|\psi(t)|^2 = 0$. This assumption is correct below threshold intensity when $(n_I^{\text{stb}})^2\kappa < P_{\text{th}} = \gamma_C\gamma_R/R$, or above threshold at the initial stage of the system evolution (stage I), when polariton density is still negligibly small in comparison to the reservoir density. The active reservoir Eqs. (4) has the analytic solution

$$n_R(t) = -\frac{(n_I^{\text{stb}})^2\kappa}{\gamma_R}(e^{-\gamma_R t} - 1), \quad (8)$$

where the characteristic level of the stationary density is

$$n_R^0 = \frac{P_I}{\gamma_R}, \quad (9)$$

where $P_I = (n_I^{\text{stb}})^2 \kappa$ describes the effective pumping intensity generated by the inactive reservoir. On the other hand, as follows from Eqs. (4), above threshold $P_I > P_{\text{th}}$ when the condensate density achieves the stationary level, the reservoir density is equal to

$$n_R^C = \frac{\gamma_C}{R}. \quad (10)$$

We can introduce the Δn parameter describing the difference between reservoirs level in the case of the condensate absence n_R^0 and presence n_R^C

$$\Delta n = \frac{P_I - P_{\text{th}}}{\gamma_R}. \quad (11)$$

The value of this parameter can be connected to the amplitude of the oscillations of the active reservoir. In the case of large Δn , stabilization of the condensate density is accompanied by noticeable oscillations.

In the case of excitation of the system with an ultrashort optical pulse, we assume that time evolution starts just after the arrival of the pulse. The pulse generates a certain density of the inactive reservoir $n_I(0) = n_I^{\text{in}}$ at $t = 0$. The relaxation and decay of the inactive reservoir density is described by

$$\frac{d}{dt} n_I(t) = -\kappa n_I(t)^2 - \gamma_I n_I(t). \quad (12)$$

The above equation has the analytical solution

$$n_I(t) = \frac{\gamma_I n_I^{\text{in}}}{(\kappa n_I^{\text{in}} + \gamma_I) \exp(\gamma_I t) - \kappa n_I^{\text{in}}}. \quad (13)$$

This equation describes the quasiexponential decay of the inactive reservoir population. Note that it is independent of the active reservoir and condensate density.

B. Condensate dynamics

In this subsection, we analyze the full dynamics of the system, including the polariton condensate. We present nontrivial oscillatory dynamics resulting from the coupling between the active reservoir and the condensate.

Our starting point is the set of evolution equations in the single mode approximation, Eqs. (4). To demonstrate the qualitative properties of its solutions, we note that the inactive reservoir is not influenced by the other two components. Moreover, its dynamics in the oscillatory stage are typically slow, both in the case of pulsed and continuous wave excitation. This is due to the small decay rate γ_I , which physically is related to the low probability of radiative recombination of high energy excitations. Therefore, for qualitative analysis, it is reasonable to approximate the inactive reservoir density by a constant value. In the case of continuous wave excitation, it is equal to the stationary value given by Eq. (7), while in the pulsed excitation case it is the instantaneous value of n_I , which is assumed to decay very slowly. We combine the two remaining equations of the set Eqs. (4) for n_C and n_R to

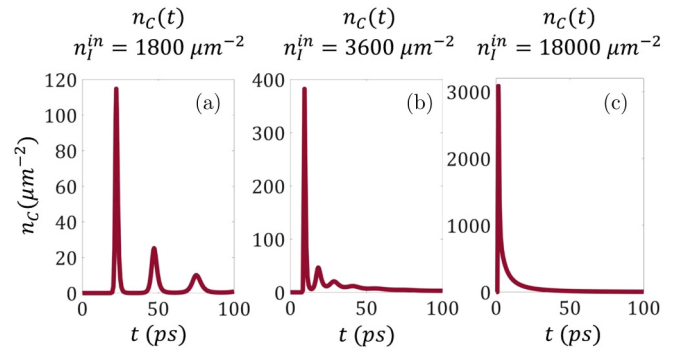


FIG. 2. Evolution of polariton condensate density under ultra-short pulsed excitation. The above three panels show, respectively, (a) spiked pulse emission, (b) decaying harmoniclike oscillations, and (c) smooth stabilization. Simulation parameters are given in Table I.

obtain the second-order equation for the evolution of polariton density:

$$\frac{d^2 n_C}{dt^2} = -(\gamma_C \gamma_R + \gamma_C R n_C(t) - P_I R) n_C - (R n_C(t) + \gamma_R) \frac{dn_C}{dt} + \frac{\left(\frac{d}{dt} n_C(t)\right)^2}{n_C(t)}, \quad (14)$$

where $P_I = n_I^2 \kappa$. The above form of the equation suggests that the solutions may have the form similar to those of a damped harmonic oscillator. However, we note that this is not the case in the low polariton density limit. Indeed, it is straightforward to show that in the linear limit of $n_C \rightarrow 0$ and with the substitution $x = \dot{n}_C/n_C$ the above equation reduces to

$$\dot{x} = -Ax - B, \quad (15)$$

where A and B are constants, which has an exponentially decaying solution. Therefore, any oscillatory behavior may only occur in the nonlinear regime, where the second-order terms in n_C in Eq. (14) provide qualitative corrections to the dynamics. The more detailed mathematical analysis of the nonlinear regime is presented in the next subsection.

To demonstrate the character of complex oscillatory dynamics of the system, we present the evolution described by the full model Eqs. (4). The typical evolution of condensate density is presented in Fig. 2, showing (a) the spiked pulsed emission, (b) decaying oscillations, and (c) quasiexponential decay. Note that all three behaviors were observed in experiments [28,30]. The evolution in a three-dimensional phase space in the case of Fig. 2(a) is presented in Fig. 3(a). The spiral corresponds to the periodic behavior of the system, with a gradually decaying inactive reservoir density n_I . In Fig. 3(b), we present a cross-section of phase space corresponding to the blue surface in Fig. 3(a). The arrows correspond to the gradient of the evolution in the (n_C, n_R) subspace at the time when the value of n_I is equal to the $1000 \mu\text{m}^{-2}$. The orange dot is the center of the spiral, which is a stationary point within the subspace. In this case, instead of vibrations around a stationary path in phase space, large-amplitude pulsations occur as the condensate density intermittently decreases to zero. The phase space evolution is characterized by a spiral

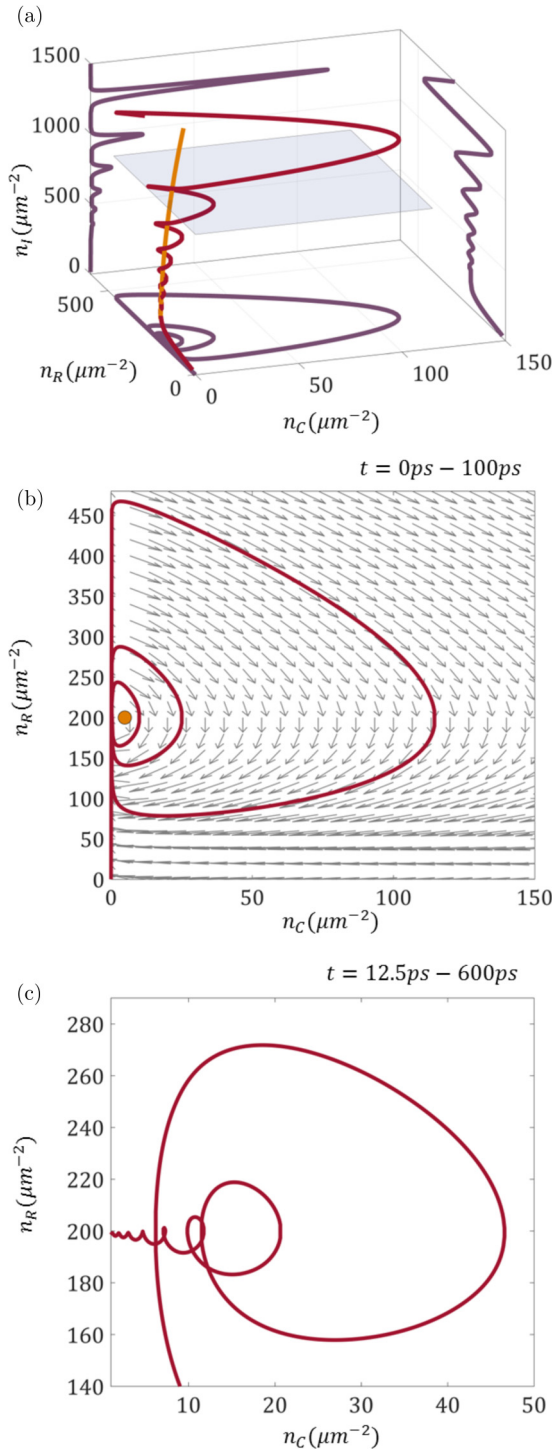


FIG. 3. (a) Phase space of trajectory in the pulsed excitation case of Fig. 2(a) (red line). Purple lines correspond to the evolution projected, respectively, to (n_I, n_C) , (n_I, n_R) , and (n_R, n_C) subspaces. The spiral evolution corresponds to the oscillatory behavior of the system, with a gradually decaying inactive reservoir density n_I . It follows the evolution of the stationary state at a particular value of n_I (orange line). (b) Cross-section of the phase space corresponding to the blue surface in panel (a). The arrows indicate the gradient of the evolution in the (n_C, n_R) subspace at the time when the value of n_I is equal to $1000 \mu\text{m}^{-2}$. The orange dot is the center of the spiral, which is a stationary point within this subspace. (c) Same as (b) but in the case of decaying harmoniclike oscillations of Fig. 2(b).

flattened at the $n_C = 0$ axis. A spiral of different dynamics is presented in Fig. 3(c) and corresponds to the decaying oscillations of Fig. 2(b). The evolution is essentially different than the pulsed spiked dynamics, especially evident in the spiral shape in the cross-section. In this case, the amplitude of oscillations decreases in time, which is the reason for convergence of the phase space trajectory. Additionally, reservoir density is characterized with small oscillations around the reservoir stabilization level.

The remarkable characteristic of the oscillatory dynamics is the change of the character of the solution type from exponential to oscillatory in the subsequent stages of the evolution. These qualitative changes in the dynamics are related to bifurcations and are analyzed in the next section.

IV. FIXED POINT ANALYSIS

In this subsection, we analyze the fixed points of Eq. (14) and determine the character of solutions around these points in the approximation of small perturbations. Such analysis is well suited for the description of solutions of nonlinear differential equations. These investigation adapted to the obtained nonlinear polariton equation allows us to determine the analytical condition for oscillations by classification of fixed points which generally can be a spiral, a center, a saddle, or a stable/unstable node [39].

We rewrite Eq. (14) in the form

$$\begin{cases} \dot{X} = f(Y) \\ \dot{Y} = g(X, Y), \end{cases} \quad (16)$$

where $X = n_C(t)$ and $Y = \frac{d}{dt}n_C(t)$, which results in

$$\begin{cases} \dot{X} = Y, \\ \dot{Y} = -(\gamma_C \gamma_R + \gamma_C R X - P_I R) X \\ \quad - (R X + \gamma_R) Y + \frac{Y^2}{X}. \end{cases} \quad (17)$$

We consider the phase portrait in the vicinity of fixed points (X^*, Y^*) , which fulfill the conditions $f(X^*, Y^*) = 0$ and $g(X^*, Y^*) = 0$.

Equation (17) is characterized by two fixed points (X_1^*, Y_1^*) and (X_2^*, Y_2^*) . The first point $Y_1^* = 0$, $X_1^* = 0$ corresponds to the absence of condensate in the system. As we demonstrated in the previous section, in the vicinity of this point, i.e., in the limit $n_C \rightarrow 0$, the system cannot display any oscillatory dynamics as the evolution has the character of a smooth decay described by Eq. (15).

An important consequence of the absence of oscillations around (X_1^*, Y_1^*) is that they cannot appear in the model with only one reservoir, in the case of pulsed excitation. Indeed, consider the following simplified model:

$$\begin{aligned} \frac{dn_C}{dt} &= R n_R n_C - \gamma_C n_C, \\ \frac{dn_R}{dt} &= P(t) - \gamma_R n_R - R n_R n_C, \end{aligned} \quad (18)$$

where we removed the inactive reservoir and replaced the scattering term with direct pumping $P(t)$. After arrival of the pumping pulse, this system would follow the evolution given by the above equation with $P(t > 0) = 0$, which does not possess the nontrivial fixed point (X_2^*, Y_2^*) . Therefore,

the second, inactive reservoir is crucial for the existence of relaxation oscillations in the pulsed excitation case. Note that in the continuous wave excitation case, the second reservoir is not crucial for the existence of oscillations since the continuous external pumping would have the same effect as the nonzero P_I term in the full set of equations. The second fixed point $Y_2^* = 0$ and $X_2^* = (P_I - P_{th})/(\gamma_C)$ corresponds to the above-threshold ($P_I > P_{th}$) stationary solution achieved when the condensate is stabilized, and it will be considered below. We can classify the different types of system dynamics using linearization around (X_2^*, Y_2^*) . This technique can reveal the phase portrait near the fixed point and determine their type [39]. We introduce a small perturbation given by $u = X - X^*$ and $v = Y - Y^*$, with $\dot{u} = \dot{X}$ and $\dot{v} = \dot{Y}$. Using Taylor series expansion we rewrite Eq. (17) in the form

$$\begin{cases} \dot{u} = u \frac{\partial f}{\partial X} + v \frac{\partial f}{\partial Y} + O(u^2, v^2, uv) \\ \dot{v} = u \frac{\partial g}{\partial X} + v \frac{\partial g}{\partial Y} + O(u^2, v^2, uv), \end{cases} \quad (19)$$

where the derivatives are taken at (X_2^*, Y_2^*) . The perturbation (u, v) evolves as

$$\begin{pmatrix} \dot{u} \\ \dot{v} \end{pmatrix} \approx \mathbf{A} \begin{pmatrix} u \\ v \end{pmatrix}, \quad (20)$$

where we neglected second-order terms and \mathbf{A} is the Jacobian matrix

$$\mathbf{A} = \begin{pmatrix} \frac{\partial f}{\partial X} & \frac{\partial f}{\partial Y} \\ \frac{\partial g}{\partial X} & \frac{\partial g}{\partial Y} \end{pmatrix}_{|(X^*, Y^*)}. \quad (21)$$

We find the eigenvalues of the problem λ

$$\lambda_{(X^*, Y^*)}^{I, II} = \frac{\tau_{(X^*, Y^*)} \pm \sqrt{\tau_{(X^*, Y^*)}^2 - 4\Delta_{(X^*, Y^*)}}{2}, \quad (22)$$

where τ and Δ are the trace and the determinant of the Jacobian, respectively, given by

$$\tau = -RX^* - \gamma_R + \frac{2Y^*}{X^*}, \quad (23)$$

$$\Delta = -RP_I + 2\gamma_C R X^* + \gamma_C \gamma_R + R Y^* + \frac{Y^{*2}}{X^{*2}}. \quad (24)$$

The solution of Eq. (22) can be real or complex. The full diagram of possible fixed points is presented in Fig. 4. In the case when the eigenvalues are complex, the fixed point is a stable spiral which attracts trajectories surrounding it while they perform oscillations. Such trajectories are similar to damped harmonic oscillations, and in our case spirals correspond to relaxation oscillations. On the other hand, when the eigenvalues are real, the evolution is a simple exponential decay and there are no oscillations.

Substituting Eqs. (23) and (24) into Eq. (22) and substituting the analytical form of (X_2^*, Y_2^*) , we obtain the analytical condition for relaxation oscillations given by the square root of $\tau_{(X_2^*, Y_2^*)}^2 - 4\Delta_{(X_2^*, Y_2^*)}$:

$$(RP_I)^2 - 4\gamma_C^2 R(P_I - P_{th}) > 0, \quad (25)$$

which determines whether the fixed point is a stable spiral or a stable node. When the above relation is fulfilled, condensate

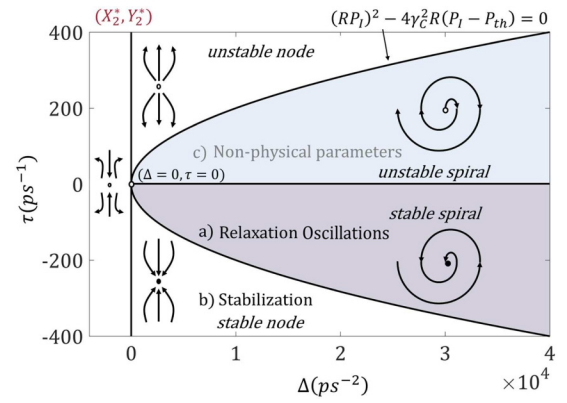


FIG. 4. Schematic presentation of the types of fixed points. The figure axes correspond to the trace τ and the determinant Δ of the Jacobian \mathbf{A} . The bold black line corresponds to the analytical condition for relaxation oscillations.

evolution is characterized by relaxation oscillations, as the fixed point is a stable spiral.

The analytical condition for relaxation oscillations Eq. (25) and the equation for the inactive reservoir stationary density Eq. (7) allow for the determination of a diagram in parameter space, presented in Fig. 5, together with typical system dynamics. For continuous wave excitation and fixed parameters R and γ_R , the region in parameter space corresponding to oscillations is broader for a short polariton lifetime, which means that this phenomenon should be pronounced for relatively low-quality samples with short polariton lifetimes, as shown in phase diagram at the bottom of Fig. 5. The oscillations can have the character of spiked pulsations as in Fig. 5(a) and, at higher pumping power, quickly decaying oscillations as in Fig. 5(b). Nevertheless, even for long polariton lifetime, oscillations can be observed at low pumping. These observations are in qualitative agreement with the experimental data presented in Ref. [28].

When the relation Eq. (25) is not fulfilled, the condensate stabilizes at a stationary level without oscillations, which is presented in Figs. 5(c) and 5(d). In the case of Fig. 5(c), condensate density increases rapidly and then relaxes to a steady state without oscillations. The peak of condensate intensity is due to the high ratio of P/P_{th} . In Fig. 5(d), polariton condensate saturates slowly and stabilizes at a stationary value.

In the case of pulsed excitation, presented in Fig. 6, the character of oscillations can be determined only for a given value of $n_I(t)$, which is assumed to change slowly in time. Consequently, during the evolution, the system may evolve from exponential decay, through oscillatory, and back to exponential stage. This is illustrated in Fig. 6(a), where the paths of evolution corresponding to Fig. 2 are marked. While all the paths go through the oscillatory region, the evolutions in Figs. 2(a)–2(c) are markedly different. In particular, in Fig. 2(c) there are no visible oscillations. This behavior can be explained by analysis of the trajectory in the full phase space in Fig. 6(b). Before reaching the oscillatory region, the system “sticks” to the stationary state through relaxation in the stable regime. In subsequent evolution, the system is very close to this state, which makes the oscillations unobservable. In this

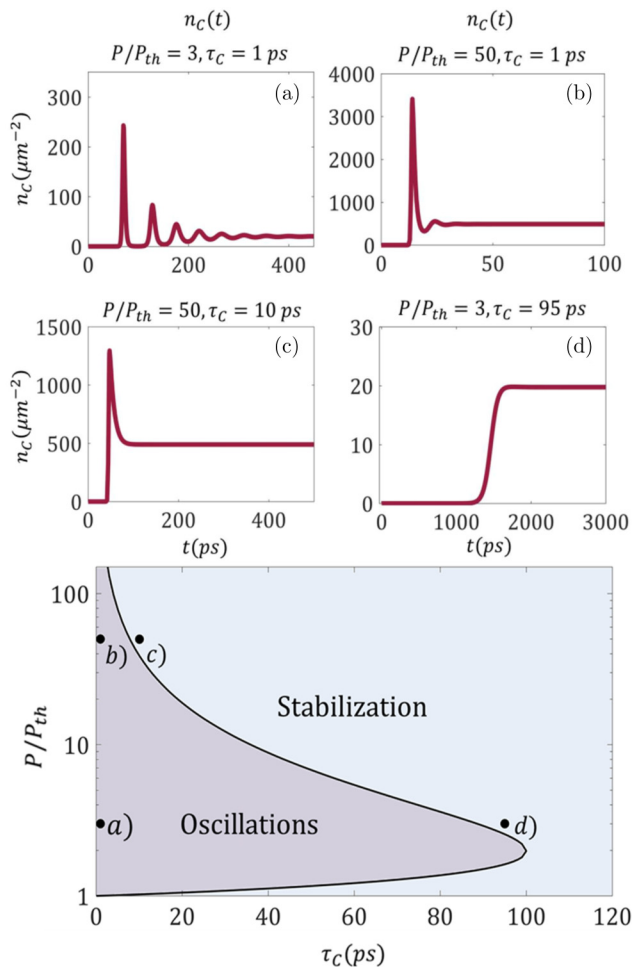


FIG. 5. Bottom: Diagram showing region in parameter space which exhibits oscillations in the case of continuous wave excitation, according to the analytical formula, Eq. (25). (a)–(d) Examples of evolutions of condensate density corresponding to the points marked in the diagram.

sense, extremely small oscillations of polariton field exist, continuously changing the amplitude around a steady point.

In contrast, the spiked pulsed emission of Fig. 2(a) can be understood as the result of a large deviation of the initial state from the stationary state in this case. The oscillations in parameter space are so large in amplitude that they no longer have a harmonic character but are characterized by periods of complete disappearance of the condensate density, as shown in Fig. 3(b).

The above considerations indicate that the range in parameter space which correspond to oscillations is mostly placed in the short polariton lifetime region. A similar condition has been previously determined for the polariton condensate instability in the case of continuous nonresonant pumping [14]. Both oscillations and instability appear to be related to the nonadiabaticity of the evolution, when the active reservoir and condensate density cannot be reduced to a single degree of freedom [40]. This instability was recently observed in Refs. [14] and [41]. However, we note that the two phenomena are very different, which is clear from the fact that the instability relies on the polariton-reservoir interactions, while in the

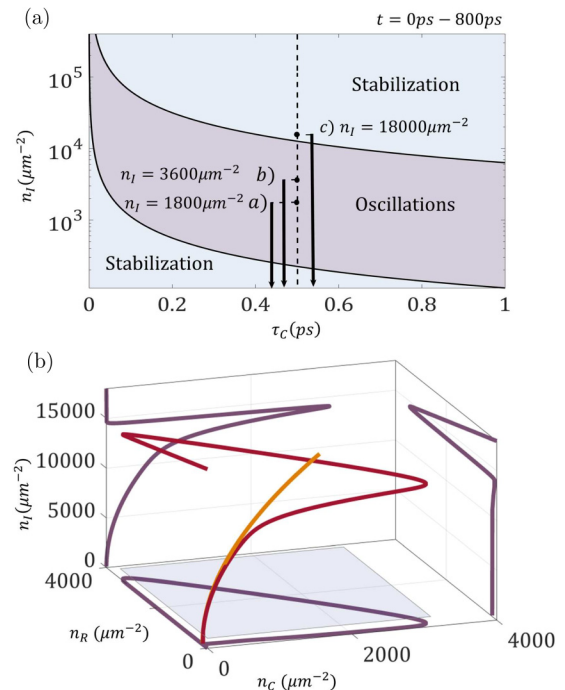


FIG. 6. (a) Diagram similar to Fig. 5, but in the case of pulsed excitation. Here, instead of power P/P_{th} , we plot the inactive reservoir density, which decays slowly during the evolution. The arrows indicate the paths in parameter space corresponding to the panels in Fig. 2. While all evolutions traverse the oscillatory region, in the case (c) there are no visible oscillations because the system “sticks” to the stationary state while passing through it, as shown in panel (b).

description of relaxation oscillations the effect of interactions can be neglected on the level of Eqs. (4).

V. CONCLUSION

In conclusion, we studied relaxation oscillations in an exciton-polariton condensate analytically and numerically using a model including both active and inactive reservoir. We derived a second-order differential equation for condensate density, applicable in the regime of continuous wave excitation or pulsed excitation provided that inactive reservoir is decaying slowly. We investigated the properties of fixed points of the equation and concluded that oscillations can occur only around the nontrivial second fixed point which appears in the nonlinear regime. We derived an analytical condition for the appearance of oscillations consistent both with numerical simulations and with previous experimental observations. We demonstrated that oscillatory behavior should be observable mainly in low quality microcavities, i.e., having short photon lifetimes. Additionally, we presented regimes of oscillating and spiked pulsating dynamics, and described the corresponding trajectories in the phase space.

ACKNOWLEDGMENTS

We acknowledge support from the National Science Centre, Poland, Grants No. 2015/17/B/ST3/02273, No. 2016/22/E/ST3/00045, and No. 2016/23/N/ST3/01350.

APPENDIX

Below, we present the parameters used in the numerical simulations, summarized in Table I.

TABLE I. Parameters used in simulations to obtain the results presented in this paper. Note that some parameters are given directly in the figures.

Figures	Fig. 1	Figs. 2, 3, and 6	Fig. 5	
τ_C	2	0.5	-	ps
τ_R	40	800	100	ps
τ_I	1000	2000	1000	ps
R	$8 \cdot 10^{-3}$	10^{-2}	10^{-3}	$\frac{\mu\text{m}^2}{\text{ps}}$
κ	$5 \cdot 10^{-2}$	10^{-5}	$5 \cdot 10^{-2}$	$\frac{\mu\text{m}^2}{\text{ps}}$
P	1.25	-	-	P_{th}

- [1] H. Deng, H. Haug, and Y. Yamamoto, *Rev. Mod. Phys.* **82**, 1489 (2010).
- [2] I. Carusotto and C. Ciuti, *Rev. Mod. Phys.* **85**, 299 (2013).
- [3] E. A. Ostrovskaya, J. Abdullaev, A. S. Desyatnikov, M. D. Fraser, and Y. S. Kivshar, *Phys. Rev. A* **86**, 013636 (2012).
- [4] K. G. Lagoudakis, F. Manni, B. Pietka, M. Wouters, T. C. H. Liew, V. Savona, A. V. Kavokin, R. André, and B. Deveaud-Plédran, *Phys. Rev. Lett.* **106**, 115301 (2011).
- [5] Y. V. Kartashov and D. V. Skryabin, *Optica* **3**, 1228 (2016).
- [6] D. D. Solnyshkov, O. Bleu, B. Teklu, and G. Malpuech, *Phys. Rev. Lett.* **118**, 023901 (2017).
- [7] D. V. Skryabin, Y. V. Kartashov, O. A. Egorov, M. Sich, J. K. Chana, L. E. Tapia Rodriguez, P. M. Walker, E. Clarke, B. Royall, M. S. Skolnick, and D. N. Krizhanovskii, *Nat. Commun.* **8**, 1554 (2017).
- [8] M. Sich, D. V. Skryabin, and D. N. Krizhanovskii, *C. R. Phys.* **17**, 908 (2016).
- [9] A. Amo, J. Lefrère, S. Pigeon, C. Adrados, C. Ciuti, I. Carusotto, R. Houdré, E. Giacobino, and A. Bramati, *Nature Physics* **5**, 805 (2009).
- [10] G. Lerario, A. Fieramosca, F. Barachati, D. Ballarini, K. S. Daskalakis, L. Dominici, M. De Giorgi, S. A. Maier, G. Gigli, S. Kéna-Cohen, and D. Sanvitto, *Nature Physics* **13**, 837 (2017).
- [11] R. Hivet, H. Flayac, D. D. Solnyshkov, D. Tanese, T. Boulier, D. Andreoli, E. Giacobino, J. Bloch, A. Bramati, G. Malpuech, and A. Amo, *Nat. Phys.* **8**, 724 (2012).
- [12] A. Opala, M. Pieczarka, N. Bobrovska, and M. Matuszewski, *Phys. Rev. B* **97**, 155304 (2018).
- [13] H. Flayac, D. D. Solnyshkov, and G. Malpuech, *Phys. Rev. B* **83**, 193305 (2011).
- [14] N. Bobrovska, M. Matuszewski, K. S. Daskalakis, S. A. Maier, and S. Kéna-Cohen, *ACS Photonics* **5**, 111 (2018).
- [15] L. Dominici, M. Petrov, M. Matuszewski, D. Ballarini, M. De Giorgi, D. Colas, E. Cancellieri, B. Silva Fernández, A. Bramati, G. Gigli, A. Kavokin, F. Laussy, and D. Sanvitto, *Nat. Commun.* **6**, 8993 (2015).
- [16] P. Miętki and M. Matuszewski, *Phys. Rev. B* **96**, 115310 (2017).
- [17] A. Dreismann, H. Ohadi, Y. del Valle-Inclan Redondo, R. Balili, Y. G. Rubo, S. I. Tsintzos, G. Deligeorgis, Z. Hatzopoulos, P. G. Savvidis, and J. J. Baumberg, *Nat. Mater.* **15**, 1074 (2016).
- [18] D. Sanvitto and S. Kéna-Cohen, *Nat. Mater.* **15**, 1061 (2016).
- [19] M. D. Fraser, S. Höfling, and Y. Yamamoto, *Nat. Mater.* **15**, 1049 (2016).
- [20] I. I. Rabi, *Phys. Rev.* **51**, 652 (1937).
- [21] C. Weisbuch, M. Nishioka, A. Ishikawa, and Y. Arakawa, *Phys. Rev. Lett.* **69**, 3314 (1992).
- [22] L. Dominici, D. Colas, S. Donati, J. P. Restrepo Cuartas, M. De Giorgi, D. Ballarini, G. Guirales, J. C. López Carreño, A. Bramati, G. Gigli, E. del Valle, F. P. Laussy, and D. Sanvitto, *Phys. Rev. Lett.* **113**, 226401 (2014).
- [23] K. G. Lagoudakis, B. Pietka, M. Wouters, R. André, and B. Deveaud-Plédran, *Phys. Rev. Lett.* **105**, 120403 (2010).
- [24] D. D. Solnyshkov, R. Johne, I. A. Shelykh, and G. Malpuech, *Phys. Rev. B* **80**, 235303 (2009).
- [25] M. Abbarchi, A. Amo, V. G. Sala, D. D. Solnyshkov, H. Flayac, L. Ferrier, I. Sagnes, E. Galopin, A. Lemaître, G. Malpuech, and J. Bloch, *Nat. Phys.* **9**, 275 (2013).
- [26] M. Wouters and I. Carusotto, *Phys. Rev. Lett.* **99**, 140402 (2007).
- [27] E. S. Sedov, Y. G. Rubo, and A. V. Kavokin, *Phys. Rev. B* **97**, 245312 (2018).
- [28] M. De Giorgi, D. Ballarini, P. Cazzato, G. Deligeorgis, S. I. Tsintzos, Z. Hatzopoulos, P. G. Savvidis, G. Gigli, F. P. Laussy, and D. Sanvitto, *Phys. Rev. Lett.* **112**, 113602 (2014).
- [29] T. Horikiri, K. Kusudo, M. D. Fraser, Y. Matsuo, A. Löffler, S. Höfling, A. Forchel, and Y. Yamamoto, *J. Phys. Soc. Jpn.* **87**, 094401 (2018).
- [30] M. Pieczarka, M. Syperek, L. Dusanowski, A. Opala, F. Langer, C. Schneider, S. Höfling, and G. Sek, *Sci. Rep.* **7**, 7094 (2017).
- [31] A. E. Siegman (ed.), *Lasers* (University Science Books, Sausalito, CA, 1986).
- [32] J. H. Shirley, *Am. J. Phys.* **36**, 949 (1968).
- [33] A. A. Andronov, A. A. Vitt, and S. E. Khaikin, *Theory of Oscillators*, Adiwes International Series in Physics (Pergamon Press, USA, 1966).
- [34] J. Grasman, in *Mathematics of Complexity and Dynamical Systems*, edited by R. A. Meyers (Springer, New York, 2011) pp. 1475–1488.

- [35] F. Veit, M. Abmann, M. Bayer, A. Löffler, S. Höfling, M. Kamp, and A. Forchel, *Phys. Rev. B* **86**, 195313 (2012).
- [36] J. Szczytko, L. Kappei, J. Berney, F. Morier-Genoud, M. T. Portella-Oberli, and B. Deveaud, *Phys. Rev. Lett.* **93**, 137401 (2004).
- [37] M. Matuszewski and E. Witkowska, *Phys. Rev. B* **89**, 155318 (2014).
- [38] P. Stepnicki and M. Matuszewski, *Phys. Rev. A* **88**, 033626 (2013).
- [39] S. H. Strogatz, *Nonlinear dynamics and Chaos: With Applications to Physics, Biology, Chemistry, and Engineering*, 2nd ed. (Westview Press, 2015), includes bibliographical references and index.
- [40] N. Bobrovska and M. Matuszewski, *Phys. Rev. B* **92**, 035311 (2015).
- [41] F. Baboux, D. D. Bernardis, V. Goblot, V. N. Gladilin, C. Gomez, E. Galopin, L. L. Gratiet, A. Lemaître, I. Sagnes, I. Carusotto, M. Wouters, A. Amo, and J. Bloch, *Optica* **5**, 1163 (2018).